Environmental Science & Technology Letters

pubs.acs.org/journal/estlcu

Letter

Light Absorption by Organic Aerosol Emissions Rivals That of Black Carbon from Residential Biomass Fuels in South Asia

Apoorva Pandey, Alice Hsu, Suresh Tiwari, Shamsh Pervez, and Rajan K. Chakrabarty*

Cite This: *Environ. Sci. Technol. Lett.* 2020, 7, 266−272

Read Online

ACCESS | Metrics & More | Article Recommendations | Supporting Information

ABSTRACT: Solid-biomass-fuel residential cookstoves are the largest source of aerosol emissions in the Indian subcontinent. For assessing radiative forcing due to this pollutant source, laboratory-generated cookstove performance data sets are currently used, which have established black carbon (BC) as the dominant atmospheric-warming aerosol species. We report findings on the strong near-ultraviolet wavelength absorption characteristics of emitted organic carbon (OC) aerosols from household stove combustion of nationally representative biomass fuels. OC emissions from cookstoves have been conventionally parametrized in regional climate models to be nonlight-absorbing in the visible solar spectra. We conclude that light-absorbing OC contributes roughly as much as BC to total absorption cross sections, thereby enhancing the associated positive forcing estimates. Our findings underscore the importance of including light-absorbing OC within the subcontinent's air quality and climate impact assessment frameworks.

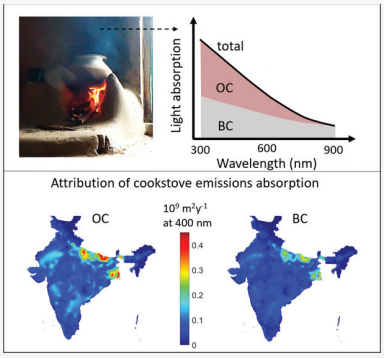

INTRODUCTION

Aerosol burden over much of the Indian subcontinent is five times higher than that over developed countries like the United States, largely because of larger emissions of primary particles and aerosol precursors.[1] This level of particulate pollution is a leading cause of disease burden[2] and could induce lower atmospheric heating rivaling that of greenhouse gases.[3] Aerosol burden over India is linked with surface dimming[4] and decrease in monsoon rainfall trends,[5] highlighting the need to target aerosols as part of the national climate policy. The knowledge of aerosol emissions characteristics like mass emission rates and optical properties for regionally significant sources is crucial for assessing source-specific aerosol radiative impacts. Biomass cookstoves are the largest source of fine particulate emissions[6−8] and ambient particulate pollution[9] in India. Most of the best available emission factors used in inventory calculations have been obtained from laboratory cookstove tests, which do not accurately reflect cookstove performance in field conditions.[6,10] Differences in burn rate and firing practice between laboratory and field settings, even for similar fuel characteristics, affect the resultant composition and mass emission factors (grams of carbon per kilogram of fuel burnt) of carbonaceous aerosols,[11−13] leading to biases in their radiative impacts. Further, discussions of the climate impacts of aerosol emissions from residential biomass use[14,15] largely include only black carbon (BC) as a light-absorbing component. Experimental observations[16−22] and recent modeling studies[23−28] indicate the potential significance of light-absorbing organic carbon (OC) to radiative forcing estimation. Estimates of aerosol radiative forcing[23−28] due to OC light absorption use parametrized or averaged OC optical properties derived from laboratory studies of controlled biomass burning. This approach, while broadly useful, requires source-linked observational validation.

In recent studies, we reported that mass emission factors of fine particulate matter (PM) from residential biomass combustion in India were 2−8 times larger than those estimated from previous laboratory studies.[12,29] Here, we present detailed particle-phase spectrophotometric analysis[19] of the spectral absorption properties of aerosols emitted from traditional mud *chulhas* and formulate key parameters necessary as input to radiative forcing algorithms: mass absorption cross sections (MAC: m^2 g^{-1} pollutant) and absorption Ångström exponents (AAE; spectral dependency of absorption in the UV−vis-IR wavelengths). We find that combustion of biomass fuels in India is the largest source of light-absorbing OC aerosols in India. Our findings highlight the significance of absorbing OC to direct radiative forcing over the region and suggest that the control of OC emissions through efficient cooking technologies could be of crucial importance to regional climate change and associated health risks mitigation.[30] Inefficient solid biomass cookstoves are used to prepare food for nearly 2.7 billion people globally:[31] the implications of this study may be applicable to other regions of

Received: January 24, 2020
Revised: March 3, 2020
Accepted: March 3, 2020
Published: March 3, 2020

https://dx.doi.org/10.1021/acs.estlett.0c00058
Environ. Sci. Technol. Lett. 2020, 7, 266−272

Asia, as well as Africa and South America, where cooking with solid biomass fuels is prevalent.

MATERIALS AND METHODS

We conducted a two-week long series of cooking tests in a rural household located on the outskirts of Raipur, in the central Indian state of Chhattisgarh. The majority (approximately 77%) of this state's households rely predominantly on solid biomass fuels for cooking.[11] Thirty cooking tests with three fuel types (fuelwood, agricultural residue, and cattle dung) were performed on a traditional mud *chulha*, which is associated with poor heat insulation and poor combustion efficiency and does not allow proper mixing of fuel and air.[32] Most Indian rural households—an estimated 150−200 million—use the traditional "mud *chulha*" for preparing their daily meals.[31] We assume that this stove type serves as a representative traditional cooking technology, although it should be noted that variations in stove design may be expected to influence emissions properties.[11,13,33,34] Fuels were sourced from different Indian states that have high biomass user populations: (a) Wood chunks were obtained from Uttar Pradesh, Rajasthan, Andhra Pradesh, Bihar, and Punjab, which collectively account for 35% of the total user base in India. (b) Cattle dung cakes were collected from Uttar Pradesh and Bihar, which account for 60% of the dung use for cooking in India. (c) Agricultural residues from *tur* crops (a type of woody stalk) and rice straw were procured from a village in Chhattisgarh. Details of the mass emission factors of aerosols (PM, BC, and OC) from the study have been presented in a previous publication.[12]

Estimation of Absorption Emission Factors. Particulate matter samples were simultaneously collected on a polytetrafluoroethylene (PTFE) membrane and quartz fiber filters (a schematic of the sampling setup is in Figure S1), during different times in each cooking cycle (to include ignition, flaming, and smoldering events). This is because combustion conditions, as typified by these events, control the optical properties of the associated PM and OC emissions.[11,20,21] Particle mass deposited was measured by weighing the PTFE filters before and after sampling, while elemental (hereafter referred to as black carbon or BC) and organic carbon mass was obtained using the IMPROVE_A thermal-optical reflectance method.[35] For each PTFE filter, transmittance and reflectance were measured for wavelengths λ in the range of 350−900 nm using a PerkinElmer LAMBDA-35 UV−vis spectrophotometer, and the relevant optical depth (OD_s) of the filter−particle system was calculated as

$$OD_s(\lambda) = \ln\left(\frac{1 - R_s(\lambda)}{T_s(\lambda)}\right) \quad (1)$$

In a recent study, we showed that OD_s is a reliable estimator of aerosol light absorption from filter optical measurements for a wide range of biomass combustion aerosols.[36] The empirical correction scheme derived in that work was used to calculate particle-phase light absorption optical depth (ABS_{PM})

$$ABS_{PM}(\lambda) = 0.48(OD_s(\lambda))^{1.32} \quad (2)$$

This dimensionless absorption parameter was converted to a cross section using the sampling area on the filter substrate and normalized by the mass of fuel consumed during the sampling period to yield absorption emission factors (AEFs)

$$AEF_{PM} = \frac{ABS_{PM} \times A_s \times CMF_{fuel}}{\Delta C_{CO_2}\left(\frac{M_c}{M_{CO_2}}\right) + \Delta C_{CO}\left(\frac{M_c}{M_{CO}}\right) \times Q \times \Delta t_s} \quad (3)$$

where A_s is the sample area (m^2) on the filter, and the last term on the right-hand side is the inverse of the mass of fuel consumed (g^{-1}). ΔC_{CO2} and ΔC_{CO} are the concentrations above ambient levels (background measured before each cooking test) of CO_2 and CO in g m^{-3}, respectively. M_C, M_{CO2}, and M_{CO} are the atomic or molecular weights of C, CO_2, and CO in g mol^{-1}, respectively. CMF_{fuel} is the carbon mass fraction of the fuel, which ranged from 33% to 50% for the tested fuels. Q is the volumetric flow rate through the filter (m^3 s^{-1}). The carbon mass balance technique was used to estimate the amount of fuel consumed during each sample collection interval, Δt_s.

Attribution of Light Absorption to OC. The particulate light absorption was attributed to BC and OC using a two-component model, which exploits the difference in the spectral absorption dependences of these components (Figure S2). It was assumed that absorption at wavelengths greater than 700 nm was due to BC (and coatings) alone. Values for the BC absorption Angstrom exponent (AAE_{BC}) were taken from modeling studies of fractal BC aggregates with nonabsorbing coatings, complemented by experimental observations: a central value of 1.2 (range: 0.9−1.5) was assumed.[37,38] OC contribution to light absorption at wavelengths smaller than 700 nm was estimated as

$$ABS_{OC}(\lambda) = ABS_{PM} - ABS_{BC} = ABS_{PM} - ABS_{PM,700}\left(\frac{\lambda}{700}\right)^{-AAE_{BC}} \quad (4)$$

Absorbances of the OC and BC components were used to calculate absorption emission factors (AEF_{OC} and AEF_{BC}, respectively), in a similar manner to the AEF_{PM} calculation above.

Mass Absorption Cross Sections. For calculating the mass absorption cross sections ($MAC_{PM/BC/OC}$), the dimensionless absorption optical depths for PM, BC, and OC were normalized by their respective mass loadings (L, g/m^2)

$$MAC_{PM/OC/BC} = ABS_{PM/OC/BC} \times \frac{1}{L_{PM/OC/BC}} \quad (5)$$

The OC contribution to forcing by cookstove emissions was isolated by calculating a MAC value for PM emissions with only BC-attributed light absorption

$$MAC_{PM,no\text{-}OC} = \frac{ABS_{BC}}{L_{PM}} = (ABS_{PM} - ABS_{OC}) \times \frac{1}{L_{PM}} = ABS_{PM}(1 - f_{OC}) \times \frac{1}{L_{PM}} \quad (6)$$

Radiative Forcing Calculations. Simple forcing efficiency (Wg^{1-} aerosol) is given by

$$SFE = -\frac{1}{4}S(\lambda)\tau_{atm}^2(1 - F_c) \times [2(1 - \alpha_s)^2\beta.MSC(\lambda) - 4\alpha_s.MAC(\lambda)] \quad (7)$$

SFE calculations were performed for a 550 nm wavelength (λ). The following atmospheric parameters were fixed: solar irradiance (S = 1370 Wm^{2-}), atmospheric transmissivity (τ_{atm}

https://dx.doi.org/10.1021/acs.estlett.0c00058
Environ. Sci. Technol. Lett. 2020, 7, 266−272

= 0.79), cloud fraction (F_c = 0.6), and surface albedo (α_s = 0.19 for ground and 0.8 for snow). Particle upscatter fraction (β) was fixed at 0.15. With the above parameters fixed, SFE is a function of MAC and mass scattering cross-section (MSC) values.

RESULTS AND DISCUSSION

Real-time measurements have shown that cookstove operation cycles consist of a series of combustion events that vary between strongly flaming and purely smoldering conditions, resulting in widely varying emissions characteristics.[11,13] Intrinsic optical properties of emitted particles are largely a function of burn conditions: previous cookstove studies observed strongly absorbing (BC-like) emissions during strongly flaming episodes and a range of weakly absorbing emissions during other phases.[11] Expectedly, AEFs in this study varied with visually observed combustion conditions: smoldering phase AEF values were lower than AEFs for steady flaming conditions (Figure 1A). The unsteady flame conditions

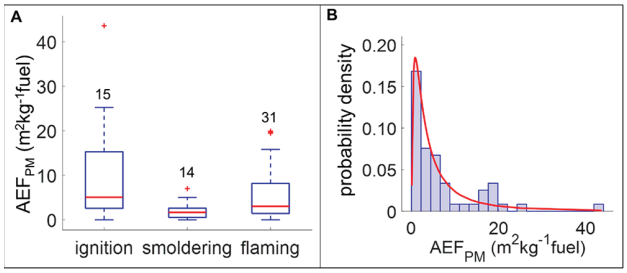

Figure 1. Particulate matter (PM) absorption emission factors, or AEF_{PM} in m^2 kg^{-1} fuel consumed, at 550 nm wavelength. (A) Grouped by observed combustion phase: boxes denote the upper and lower quartiles, and whiskers denote 1.5 times the interquartile range. Outliers are shown as red + symbols, and the number of samples for each category are specified above the whiskers. (B) Histogram of all samples, overlaid by a fitted log-normal distribution.

during the ignition phase are reflected by the large variability in ignition AEFs. Variability in burn conditions drives optical characteristics more than fuel type.[13] The differences between AEFs for the three fuel categories were statistically insignificant: on unpaired Student's *t*-test, differences between groups were not significant at p = 0.05 (see Supporting Information for statistical details). Pooled AEF data for all samples show an approximately log-normal distribution factor with a large spread. We report a combined geometric mean of 3.7 m^2 kg^{-1} fuel (and 95% confidence intervals (CI) of 0.6–23.3 m^2 kg^{-1} fuel.

Conventionally, all visible light absorption by combustion-generated aerosols in climate models was attributed to BC particles; however, the newer generation of models includes brown carbon as a light-absorbing form of OC in addition to the strongly absorbing BC.[22−24] The light-absorbing efficiencies of OC aerosols are connected to their physical and chemical properties, which in turn are a function of fuel properties and combustion conditions.[16,20,21] Optical properties and refractiveness of OC particles lie on interlinked continua: absorption efficiency and thermal stability are linked with high molecular weight organic compounds formed under flaming conditions.[16,20,21] Higher relative abundances of BC are correlated with higher light-absorbing efficiency of the coemitted OC.[21] Cookstove emissions in this study are characterized by fuel-wise average BC/OC ratios of 0.08–0.15, with the lowest BC fractions observed for dung and the highest for fuelwood. These ratios are consistent with the findings of other recent field observations of cookstove emissions.[13,39,40] However, they are on the lower end of the range (0.04–1.67) observed for laboratory cookstove tests of similar fuel types[41] but larger than those from field measurements (0.02–0.08) for open biomass burning.[42−44] Thermal carbon profiles of the emissions in this study show that thermally stable OC, that evolves at 450 °C in an inert atmosphere, constitute the largest particulate fraction (~50% of total carbon mass, on average).[12] Therefore, OC from cookstove emissions is expected to be an important contributor to visible light absorption.

By exploiting theoretical and experimental knowledge of BC optical characteristics, we attempt at apportioning the total particulate light absorption associated with cookstove emissions to its BC and OC components. BC particles emitted from biomass burning are likely to be coated with organic material that enhances light absorption with respect to pure BC. While the wavelength dependence of BC light absorption is described by an AAE of 1, modeling[38] and experimental[37] studies show that coated fractal-like BC aggregates have AAE in the range of 0.9–1.5. A central BC AAE value of 1.2 (with 0.9 and 1.5 as lower and upper extremes, respectively) was used in this study to describe BC's spectral absorption behavior. All light absorption for wavelengths larger than 700 nm was attributed to coated BC, and BC light absorption at smaller wavelengths was estimated from BC absorption at 700 nm using the above AAE values. OC light absorption is estimated as the difference between the total and coated BC absorption values (eq 4). While the true value of BC AAE for each sample is uncertain, the use of a reasonable range of BC AAE values allows us to constrain the OC contribution to light absorption. For BC AAE of 1.2, we determined the ratio of geometric mean values of OC AEF to PM AEF at 550 nm as 0.37; this ratio for different BC AAE values ranged from 0.30 to 0.41. Previous apportionment analyses of savanna wildfire smoke[17] and residential fireplace emissions[18] showed lower OC contributions to light absorption (13%–32% at 500 nm). Distributions of OC and BC AEF values and their dependence on combustion conditions at 550 nm wavelength are shown in Figure S3. At 405 nm, we calculate the geometric mean of the OC AEF value to be approximately 6 m^2 kg^{-1}, which is within the range (5–10 m^2 kg^{-1}) reported for cookstoves in Nepal.[40]

We combined our absorption emission factors with fuel use data to estimate annual light-absorbing emissions, in Gm^2 y^{-1} or 10^9 m^2 y^{-1} (Figure 2). Bottom-up biomass fuel use estimates were disaggregated at the district level[6] and multiplied by biomass-averaged AEFs. These emissions were gridded with a spatial resolution of 0.1° × 0.1°. The mean value and 95% CI for absorption cross-section emissions (AE) at 550 nm from OC were 577 (64–2266) Gm^2 y^{-1}, while those from BC were 988 (110–3897) Gm^2 y^{-1}. In contrast OC contributes more than BC to light absorption at 400 nm: corresponding AE values for OC were 2391 (266–9390) Gm^2 y^{-1}, while those for BC were 1654 (184–6100) Gm^2 y^{-1}. Such optical inventories can be used to compare sectoral contributions to light absorption by BC and OC and discern patterns in the spatial distributions of these contributions. Figure 2 demonstrates absorption emissions hotspots over the Indo-Gangetic Plain, which is associated with a higher than

https://dx.doi.org/10.1021/acs.estlett.0c00058
Environ. Sci. Technol. Lett. 2020, 7, 266–272

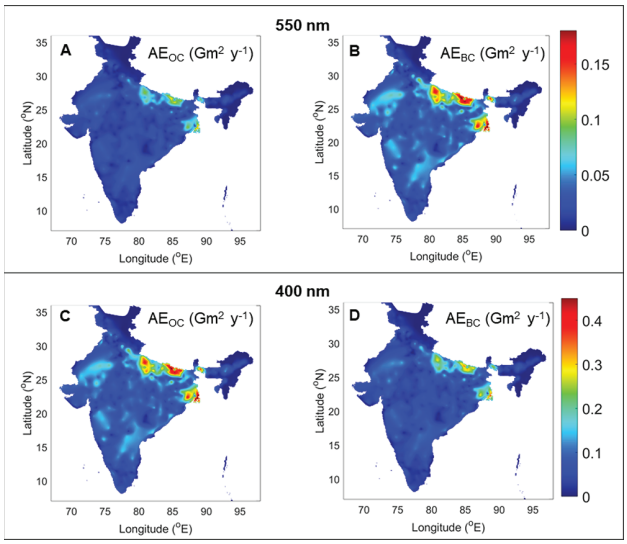

Figure 2. Spatial distribution of annual emissions expressed as light absorption cross sections (AE: Gm^2 y^{-1}) at 550 nm wavelength attributed to (A) OC and (B) BC components of cookstove emissions in India. Similar distributions at 400 nm of AE attributed to (C) OC and (D) BC. BC AAE = 1.2[37,38] was used. (Maps in this figure were generated in MATLAB R2019a. Indian administrative boundary data sets (state and district levels) were obtained from https://github.com/datameet/maps. These data are derived from Government of India sources (Census of India, Bhuvan, and Survey of India) and GeoCommons and are shared under a Creative Commons Attribution-ShareAlike 2.5 India license).

average aerosol burden[1] with a large contribution from the residential sector.[45]

Estimating the radiative impact of emissions requires optical cross sections normalized to pollutant mass. Average MAC values for OC emissions and the contribution of OC to total light absorption, integrated over solar irradiance in the 350–900 nm wavelength range, are reported in Table 1. Our estimates of MAC$_{OC}$ and AAE$_{OC}$ are in good agreement with those from bulk-phase measurements of cookstove-emitted OC (from field tests) extracted in organic solvents.[33] We further calculated PM MAC values with and without OC absorption (Figure S4) to evaluate OC contribution to direct radiative forcing by cookstove emissions. MAC$_{PM}$ values are approximately log-normally distributed with average (and 95% confidence intervals) of 0.54 (0.10–1.46) m^2 g^{-1}, consistent with values (0.4–1.5 m^2 g^{-1}) derived from *in situ* (photoacoustic) absorption measurements[46] and corresponding mass emission factors[39] of particulate matter from biomass cookstoves in Nepal. MAC$_{PM}$ values in this study are slightly smaller than those from our earlier analysis[19] on a smaller set of samples from Indian cookstove emissions, largely due to improved treatment of filter artifacts.[36] Our estimates are significantly smaller than MAC$_{PM}$ (range of 0.5–6.6 m^2 g^{-1}) calculated using other filter-based measurements of absorption from cookstove emissions in laboratory[41] or field[13,47] settings.

When OC light absorption is set to zero, MAC$_{PM,no\text{-}OC}$ can be calculated by normalizing the remaining (BC only) absorption to PM mass. This quantity depends on the assumed values of BC AAE and exhibits a log-normal distribution with a large spread. Mean values of MAC$_{PM,no\text{-}OC}$ ranged from 0.39 to 0.45 m^{2}g^{-1}. The large, overlapping ranges of MAC$_{PM}$ and MAC$_{PM,no\text{-}OC}$ pose a challenge in constraining the OC contribution to direct radiative forcing. However, these parameters do not vary independently of each other: at a 550 nm wavelength, higher absorption efficiencies of cookstove emissions are associated with a larger contribution from BC or a correspondingly smaller contribution from OC (Figure 3A). In other words, MAC$_{PM}$ and MAC$_{PM,no\text{-}OC}$ are positively correlated, and their dependence can be captured by a linear relationship (Figure 3B).

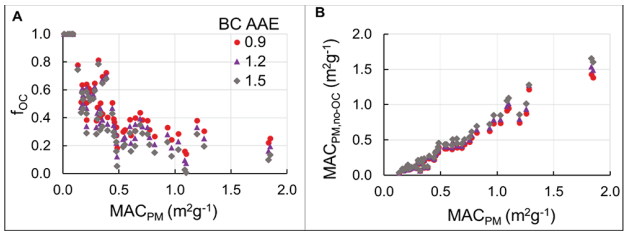

Figure 3. (A) Fractional contribution of OC light absorption to MAC$_{PM}$ at 550 nm, f_{OC}, as a function of MAC$_{PM}$. (B) Correlation between MAC$_{PM,no\text{-}OC}$ and MAC$_{PM}$. Linear fits between the two parameters are in Table S1 of the Supporting Information.

This correlation was exploited for radiative forcing efficiency calculations. MAC$_{PM}$ was sampled from the probability distribution observed (Figure S4), which was used to calculate MAC$_{PM,no\text{-}OC}$ using the linear fit parameters in Table S1. Bounds for mass scattering cross-section (MSC) values for cookstove emissions, based on measurements made from

Table 1. Simple Forcing Efficiency of Cookstove Emissions Attributed to OC Light Absorption (Wg^{-1}), MAC$_{OC}$ (m^2 g^{-1}), AAE$_{OC}$, and Contribution of OC to PM Light Absorption (Percentage of Total Absorption)[a]

		BC AAE		
		0.9	1.2	1.5
SFE attributed to OC (W g^{-1})	ground	12.1 ± 3.9	10.3 ± 2.6	8.6 ± 1.3
	snow	51.4 ± 16.9	43.9 ± 11.3	36.3 ± 5.7
MAC$_{OC}$ (m^2 g^{-1})	550 nm	0.41 ± 0.33	0.36 ± 0.26	0.29 ± 0.20
	350 nm	2.79 ± 1.89	2.53 ± 1.69	2.21 ± 1.54
AAE$_{OC}$ (350–700 nm)		5.8 ± 1.3	5.9 ± 1.3	6.0 ± 1.8
Integrated (350–900 nm) OC contribution to light absorption (%)		56 ± 26	52 ± 28	48 ± 30

[a]These estimates depend on the value of BC AAE used in absorption apportionment. All values are reported as mean ±1 standard deviation.

https://dx.doi.org/10.1021/acs.estlett.0c00058
Environ. Sci. Technol. Lett. 2020, 7, 266–272

South Asian *chulhas*,[13] were 1.5−2.5 m^2 g^{-1}. Simple forcing efficiency (SFE) was calculated as a function of MAC and MSC.[48] While the magnitude of SFE is dependent on the choice of MSC, for a fixed MSC, change in SFE due to OC light absorption (SFE_{PM}, $SFE_{PM,no\text{-}OC}$) only depends on the respective MAC values. This difference can be interpreted as the contribution of OC light absorption to forcing by cookstove emissions. OC contributions to SFE are reported as a function of the BC AAE used for absorption apportionment in Table 1. OC absorption added 8.6−12.1 Wg^{-1} to forcing over ground and 36.3−51.5 W g^{-1} to forcing over snow by fresh cookstove emissions. For MSC = 1.5 m^2 g^{-1}, SFE for PM emissions over ground was estimated as 11 ± 23 W g^{-1}. Using the mean value of this estimate, we observe that if all cookstove OC was nonabsorbing, it would purely offset BC forcing (mean net forcing efficiency = −1.1 to 2.4 W g^{-1}). Distributions of SFE estimates with and without OC absorption are shown in Figure S5, and those of SFE attributed to OC are shown in Figure S6.

Household emissions are significant contributors to ambient air pollution in south Asia.[45,49,50] Recent field evaluations of cookstove performance conducted in India,[12,33] Nepal,[39,46] and Tibet[13] show that cookstove emissions are likely much larger than previously estimated. Unsteady real-world burn cycles cause weakly flaming and smoldering combustion events, producing OC emissions much more frequently than laboratory water boiling tests.[11] The OC component of cookstove PM contributes nearly as much as BC to atmospheric light absorption. We suggest the use of MAC_{OC} = 0.3−0.5 m^2 g^{-1} at 550 nm and AAE_{OC} = 6 for fresh (at-source) emissions from traditional Indian cookstoves, including an appropriate estimate of the rate of photochemical bleaching (see ref 49 for an example). Recent studies using global radiative models that evaluated the enhancement in aerosol light absorption due to OC[19,23−25,27] assumed that a fraction (50%−66%) of the OC is light absorbing and derived the index of refraction of this component using reported absorption efficiencies of solvent-extracted OC. When normalized to the mass of all OC (as done in this work), the absorption cross sections employed in these studies ranged from 0.05 to 1.0 m^2 g^{-1} at 550 nm and 1.50 to 5.01 m^2 g^{-1} at 350 nm.

Cookstove-emitted OC has an absorption efficiency comparable to that of a "strongly absorbing" type of OC modeled in Feng et al.,[23] which was linked to shifting of the net global radiative forcing of organic aerosols from cooling to warming. Replacement of traditional cookstoves with clean technologies could mitigate aerosol-related warming in addition to reducing particulate exposure and the associated disease burden[45] in south Asia. However, if these clean technologies include advanced biomass stoves, improved laboratory testing[11] and field validation are crucial for evaluating the extent, if any, of the health and climate benefits of technology replacement. Finally, we suggest that light-absorbing OC be addressed as a distinct short-lived climate-forcing agent in the scientific consensus reports of the Intergovernmental Panel on Climate Change.[51]

■ ASSOCIATED CONTENT

Supporting Information

The Supporting Information is available free of charge at https://pubs.acs.org/doi/10.1021/acs.estlett.0c00058.

Information as mentioned in the text (PDF)

■ AUTHOR INFORMATION

Corresponding Author

Rajan K. Chakrabarty − *Department of Energy, Environmental and Chemical Engineering, Washington University in St. Louis, St. Louis, Missouri 63130, United States;* orcid.org/0000-0001-5753-9937; Email: chakrabarty@wustl.edu

Authors

Apoorva Pandey − *Department of Energy, Environmental and Chemical Engineering, Washington University in St. Louis, St. Louis, Missouri 63130, United States*

Alice Hsu − *Department of Energy, Environmental and Chemical Engineering, Washington University in St. Louis, St. Louis, Missouri 63130, United States*

Suresh Tiwari − *Indian Institute of Tropical Meteorology, Pune 411008, India*

Shamsh Pervez − *School of Studies in Chemistry, Pandit Ravishankar Shukla University, Raipur, Chhattisgarh 492010, India*

Complete contact information is available at: https://pubs.acs.org/10.1021/acs.estlett.0c00058

Notes

The authors declare no competing financial interest.

■ ACKNOWLEDGMENTS

This work was supported by the U.S. National Science Foundation (AGS-1455215 and AGS-1926817), National Aeronautics and Space Administration Radiation Sciences Program (NNX15AI66G), Science and Engineering Research Board (SERB), India (EMR/2015/000928), and International Center for Energy, Environment and Sustainability (InCEES) at Washington University in St. Louis. The authors thank Dr. Praveen Kumar, currently at Boston College, for his help with fuel and sample collection. The authors also acknowledge the assistance provided in aerosol sampling and analysis by Madhuri Verma, Rakesh Sahu, and Jeevan Matawale from Pandit Ravishankar Shukla University under the mentorship of Dr. Shamsh Pervez.

■ REFERENCES

(1) David, L. M.; Ravishankara, A.; Kodros, J. K.; Venkataraman, C.; Sadavarte, P.; Pierce, J. R.; Chaliyakunnel, S.; Millet, D. B. Aerosol optical depth over India. *J. Geophys. Res.: Atmos.* **2018**, *123* (7), 3688−3703.

(2) Murray, C. J.; Vos, T.; Lozano, R.; Naghavi, M.; Flaxman, A. D.; Michaud, C.; Ezzati, M.; Shibuya, K.; Salomon, J. A.; Abdalla, S.; et al. Disability-adjusted life years (DALYs) for 291 diseases and injuries in 21 regions, 1990−2010: a systematic analysis for the Global Burden of Disease Study 2010. *Lancet* **2012**, *380* (9859), 2197−2223.

(3) Ramanathan, V.; Ramana, M. V.; Roberts, G.; Kim, D.; Corrigan, C.; Chung, C.; Winker, D. Warming trends in Asia amplified by brown cloud solar absorption. *Nature* **2007**, *448* (7153), 575−578.

(4) Kambezidis, H.; Kaskaoutis, D.; Kharol, S. K.; Moorthy, K. K.; Satheesh, S.; Kalapureddy, M.; Badarinath, K.; Sharma, A. R.; Wild, M. Multi-decadal variation of the net downward shortwave radiation over south Asia: The solar dimming effect. *Atmos. Environ.* **2012**, *50*, 360−372.

(5) Krishnan, R.; Sabin, T.; Vellore, R.; Mujumdar, M.; Sanjay, J.; Goswami, B.; Hourdin, F.; Dufresne, J.-L.; Terray, P. Deciphering the desiccation trend of the South Asian monsoon hydroclimate in a warming world. *Climate Dynamics* **2016**, *47* (3−4), 1007−1027.

(6) Pandey, A.; Sadavarte, P.; Rao, A. B.; Venkataraman, C. Trends in multi-pollutant emissions from a technology-linked inventory for India: II. Residential, agricultural and informal industry sectors. *Atmos. Environ.* **2014**, *99*, 341−352.
(7) Janssens-Maenhout, G.; Crippa, M.; Guizzardi, D.; Dentener, F.; Muntean, M.; Pouliot, G.; Keating, T.; Zhang, Q.; Kurokawa, J.; Wankmüller, R.; et al. HTAP_v2. 2: a mosaic of regional and global emission grid maps for 2008 and 2010 to study hemispheric transport of air pollution. *Atmos. Chem. Phys.* **2015**, *15* (19), 11411−11432.
(8) Kurokawa, J.; Ohara, T.; Morikawa, T.; Hanayama, S.; Janssens-Maenhout, G.; Fukui, T.; Kawashima, K.; Akimoto, H. Emissions of air pollutants and greenhouse gases over Asian regions during 2000−2008: Regional Emission inventory in ASia (REAS) version 2. *Atmos. Chem. Phys.* **2013**, *13* (21), 11019−11058.
(9) Philip, S.; Martin, R. V.; van Donkelaar, A.; Lo, J. W.-H.; Wang, Y.; Chen, D.; Zhang, L.; Kasibhatla, P. S.; Wang, S.; Zhang, Q.; et al. Global chemical composition of ambient fine particulate matter for exposure assessment. *Environ. Sci. Technol.* **2014**, *48* (22), 13060−13068.
(10) Bond, T. C.; Doherty, S. J.; Fahey, D.; Forster, P.; Berntsen, T.; DeAngelo, B.; Flanner, M.; Ghan, S.; Kärcher, B.; Koch, D.; et al. Bounding the role of black carbon in the climate system: A scientific assessment. *J. Geophys. Res. Atmos.* **2013**, *118* (11), 5380−5552.
(11) Chen, Y.; Roden, C. A.; Bond, T. C. Characterizing biofuel combustion with patterns of real-time emission data (PaRTED). *Environ. Sci. Technol.* **2012**, *46* (11), 6110−6117.
(12) Pandey, A.; Patel, S.; Pervez, S.; Tiwari, S.; Yadama, G.; Chow, J. C.; Watson, J. G.; Biswas, P.; Chakrabarty, R. K. Aerosol emissions factors from traditional biomass cookstoves in India: insights from field measurements. *Atmos. Chem. Phys.* **2017**, *17* (22), 13721−13729.
(13) Weyant, C. L.; Chen, P.; Vaidya, A.; Li, C.; Zhang, Q.; Thompson, R.; Ellis, J.; Chen, Y.; Kang, S.; Shrestha, G. R. Emission measurements from traditional biomass cookstoves in South Asia and Tibet. *Environ. Sci. Technol.* **2019**, *53*, 3306.
(14) Venkataraman, C.; Habib, G.; Eiguren-Fernandez, A.; Miguel, A.; Friedlander, S. Residential biofuels in South Asia: carbonaceous aerosol emissions and climate impacts. *Science* **2005**, *307* (5714), 1454−1456.
(15) Grieshop, A. P.; Marshall, J. D.; Kandlikar, M. Health and climate benefits of cookstove replacement options. *Energy Policy* **2011**, *39* (12), 7530−7542.
(16) Andreae, M.; Gelencsér, A. Black carbon or brown carbon? The nature of light-absorbing carbonaceous aerosols. *Atmos. Chem. Phys.* **2006**, *6* (10), 3131−3148.
(17) Kirchstetter, T. W.; Novakov, T.; Hobbs, P. V. Evidence that the spectral dependence of light absorption by aerosols is affected by organic carbon. *J. Geophys. Res.: Atmos.* **2004**, *109* (D21), n/a.
(18) Kirchstetter, T. W.; Thatcher, T. Contribution of organic carbon to wood smoke particulate matter absorption of solar radiation. *Atmos. Chem. Phys.* **2012**, *12* (14), 6067−6072.
(19) Pandey, A.; Pervez, S.; Chakrabarty, R. K. Filter-based measurements of UV−vis mass absorption cross sections of organic carbon aerosol from residential biomass combustion: Preliminary findings and sources of uncertainty. *J. Quant. Spectrosc. Radiat. Transfer* **2016**, *182*, 296−304.
(20) Saleh, R.; Cheng, Z.; Atwi, K. The brown−black continuum of light-absorbing combustion aerosols. *Environ. Sci. Technol. Lett.* **2018**, *5* (8), 508−513.
(21) Saleh, R.; Robinson, E. S.; Tkacik, D. S.; Ahern, A. T.; Liu, S.; Aiken, A. C.; Sullivan, R. C.; Presto, A. A.; Dubey, M. K.; Yokelson, R. J.; et al. Brownness of organics in aerosols from biomass burning linked to their black carbon content. *Nat. Geosci.* **2014**, *7* (9), 647−650.
(22) Chung, C. E.; Ramanathan, V.; Decremer, D. Observationally constrained estimates of carbonaceous aerosol radiative forcing. *Proc. Natl. Acad. Sci. U. S. A.* **2012**, *109* (29), 11624−11629.
(23) Feng, Y.; Ramanathan, V.; Kotamarthi, V. Brown carbon: a significant atmospheric absorber of solar radiation? *Atmos. Chem. Phys.* **2013**, *13* (17), 8607−8621.
(24) Wang, X.; Heald, C.; Ridley, D.; Schwarz, J.; Spackman, J.; Perring, A.; Coe, H.; Liu, D.; Clarke, A. Exploiting simultaneous observational constraints on mass and absorption to estimate the global direct radiative forcing of black carbon and brown carbon. *Atmos. Chem. Phys.* **2014**, *14* (20), 10989−11010.
(25) Jo, D. S.; Park, R. J.; Lee, S.; Kim, S.-W.; Zhang, X. A global simulation of brown carbon: implications for photochemistry and direct radiative effect. *Atmos. Chem. Phys.* **2016**, *16* (5), 3413−3432.
(26) Saleh, R.; Marks, M.; Heo, J.; Adams, P. J.; Donahue, N. M.; Robinson, A. L. Contribution of brown carbon and lensing to the direct radiative effect of carbonaceous aerosols from biomass and biofuel burning emissions. *J. Geophys. Res.: Atmos.* **2015**, *120* (19), 10285−10296.
(27) Wang, X.; Heald, C. L.; Liu, J.; Weber, R. J.; Campuzano-Jost, P.; Jimenez, J. L.; Schwarz, J. P.; Perring, A. E. Exploring the observational constraints on the simulation of brown carbon. *Atmos. Chem. Phys.* **2018**, *18*, 635.
(28) Brown, H.; Liu, X.; Feng, Y.; Jiang, Y.; Wu, M.; Lu, Z.; Wu, C.; Murphy, S.; Pokhrel, R. Radiative Effect and Climate Impacts of Brown Carbon with the Community Atmosphere Model (CAM5). *Atmos. Chem. Phys.* **2018**, *18*, 17745−17768.
(29) Pervez, S.; Verma, M.; Tiwari, S.; Chakrabarty, R. K.; Watson, J. G.; Chow, J. C.; Panicker, A. S.; Deb, M. K.; Siddiqui, M. N.; Pervez, Y. F. Household solid fuel burning emission characterization and activity levels in India. *Sci. Total Environ.* **2019**, *654*, 493−504.
(30) Lacey, F. G.; Henze, D. K.; Lee, C. J.; van Donkelaar, A.; Martin, R. V. Transient climate and ambient health impacts due to national solid fuel cookstove emissions. *Proc. Natl. Acad. Sci. U. S. A.* **2017**, *114* (6), 1269−1274.
(31) Khandelwal, M.; Hill, M. E., Jr; Greenough, P.; Anthony, J.; Quill, M.; Linderman, M.; Udaykumar, H. Why have improved cookstove initiatives in India failed? *World Development* **2017**, *92*, 13−27.
(32) Venkataraman, C.; Sagar, A.; Habib, G.; Lam, N.; Smith, K. The Indian national initiative for advanced biomass cookstoves: the benefits of clean combustion. *Energy Sustainable Dev.* **2010**, *14* (2), 63−72.
(33) Fleming, L. T.; Lin, P.; Laskin, A.; Laskin, J.; Weltman, R.; Edwards, R. D.; Arora, N. K.; Yadav, A.; Meinardi, S.; Blake, D. R.; et al. Molecular composition of particulate matter emissions from dung and brushwood burning household cookstoves in Haryana, India. *Atmos. Chem. Phys.* **2018**, *18* (4), 2461−2480.
(34) Roden, C. A.; Bond, T. C.; Conway, S.; Pinel, A. B. O.; MacCarty, N.; Still, D. Laboratory and field investigations of particulate and carbon monoxide emissions from traditional and improved cookstoves. *Atmos. Environ.* **2009**, *43* (6), 1170−1181.
(35) Chow, J. C.; Watson, J. G.; Robles, J.; Wang, X. L.; Chen, L.-W. A.; Trimble, D. L.; Kohl, S. D.; Tropp, R. J.; Fung, K. K. Quality assurance and quality control for thermal/optical analysis of aerosol samples for organic and elemental carbon. *Anal. Bioanal. Chem.* **2011**, *401* (10), 3141−3152.
(36) Pandey, A.; Shetty, N. J.; Chakrabarty, R. K. Aerosol light absorption from optical measurements of PTFE membrane filter samples: sensitivity analysis of optical depth measures. *Atmos. Meas. Tech.* **2019**, *12* (2), 1365−1373.
(37) Gyawali, M.; Arnott, W. P.; Zaveri, R. A.; Song, C.; Pekour, M.; Flowers, B.; Dubey, M. K.; Setyan, A.; Zhang, Q.; Harworth, J.; et al. Evolution of multispectral aerosol optical properties in a biogenically-influenced urban environment during the CARES campaign. *Atmos. Chem. Phys. Discuss.* **2013**, *13* (3), 7113−7150.
(38) Liu, C.; Chung, C. E.; Yin, Y.; Schnaiter, M. The absorption Ångström exponent of black carbon: from numerical aspects. *Atmos. Chem. Phys.* **2018**, *18* (9), 6259−6273.
(39) Jayarathne, T.; Stockwell, C. E.; Bhave, P. V.; Praveen, P. S.; Rathnayake, C. M.; Islam, M.; Panday, A. K.; Adhikari, S.; Maharjan, R.; Goetz, J. D.; et al. Nepal Ambient Monitoring and Source Testing Experiment (NAMaSTE): emissions of particulate matter from wood- and dung-fueled cooking fires, garbage and crop residue burning, brick kilns, and other sources. *Atmos. Chem. Phys.* **2018**, *18* (3), 2259−2286.

https://dx.doi.org/10.1021/acs.estlett.0c00058
Environ. Sci. Technol. Lett. 2020, 7, 266−272

(40) Goetz, J. D.; Giordano, M. R.; Stockwell, C. E.; Christian, T. J.; Maharjan, R.; Adhikari, S.; Bhave, P. V.; Praveen, P. S.; Panday, A. K.; Jayarathne, T.; et al. Speciated online PM 1 from South Asian combustion sources−Part 1: Fuel-based emission factors and size distributions. *Atmos. Chem. Phys.* **2018**, *18* (19), 14653−14679.
(41) Habib, G.; Venkataraman, C.; Bond, T. C.; Schauer, J. J. Chemical, microphysical and optical properties of primary particles from the combustion of biomass fuels. *Environ. Sci. Technol.* **2008**, *42* (23), 8829−8834.
(42) Aurell, J.; Gullett, B. K.; Tabor, D. Emissions from southeastern US Grasslands and pine savannas: Comparison of aerial and ground field measurements with laboratory burns. *Atmos. Environ.* **2015**, *111*, 170−178.
(43) Holder, A.; Gullett, B.; Urbanski, S.; Elleman, R.; O'Neill, S.; Tabor, D.; Mitchell, W.; Baker, K. Emissions from prescribed burning of agricultural fields in the Pacific Northwest. *Atmos. Environ.* **2017**, *166*, 22−33.
(44) Strand, T.; Gullett, B.; Urbanski, S.; O'Neill, S.; Potter, B.; Aurell, J.; Holder, A.; Larkin, N.; Moore, M.; Rorig, M. Grassland and forest understorey biomass emissions from prescribed fires in the south-eastern United States−RxCADRE 2012. *Int. J. Wildland Fire* **2016**, *25* (1), 102−113.
(45) Chowdhury, S.; Dey, S.; Guttikunda, S.; Pillarisetti, A.; Smith, K. R.; Di Girolamo, L. Indian annual ambient air quality standard is achievable by completely mitigating emissions from household sources. *Proc. Natl. Acad. Sci. U. S. A.* **2019**, *116*, 10711−10716.
(46) Stockwell, C. E.; Christian, T. J.; Goetz, J. D.; Jayarathne, T.; Bhave, P. V.; Praveen, P. S.; Adhikari, S.; Maharjan, R.; DeCarlo, P. F.; Stone, E. A.; et al. Nepal Ambient Monitoring and Source Testing Experiment (NAMaSTE): emissions of trace gases and light-absorbing carbon from wood and dung cooking fires, garbage and crop residue burning, brick kilns, and other sources. *Atmos. Chem. Phys.* **2016**, *16* (17), 11043−11081.
(47) Roden, C. A.; Bond, T. C.; Conway, S.; Pinel, A. B. O. Emission factors and real-time optical properties of particles emitted from traditional wood burning cookstoves. *Environ. Sci. Technol.* **2006**, *40* (21), 6750−6757.
(48) Bond, T. C.; Bergstrom, R. W. Light absorption by carbonaceous particles: An investigative review. *Aerosol Sci. Technol.* **2006**, *40* (1), 27−67.
(49) Dasari, S.; Andersson, A.; Bikkina, S.; Holmstrand, H.; Budhavant, K.; Satheesh, S.; Asmi, E.; Kesti, J.; Backman, J.; Salam, A.; et al. Photochemical degradation affects the light absorption of water-soluble brown carbon in the South Asian outflow. *Science advances* **2019**, *5* (1), No. eaau8066.
(50) Rooney, B.; Zhao, R.; Wang, Y.; Bates, K. H.; Pillarisetti, A.; Sharma, S.; Kundu, S.; Bond, T. C.; Lam, N. L.; Ozaltun, B.; et al. Impacts of household sources on air pollution at village and regional scales in India. *Atmos. Chem. Phys.* **2019**, *19* (11), 7719−7742.
(51) *Climate Change 2014: Synthesis Report*. Contribution of Working Groups I, II and III to the Fifth Assessment Report of the Intergovernmental Panel on Climate Change, 2014.

https://dx.doi.org/10.1021/acs.estlett.0c00058
Environ. Sci. Technol. Lett. 2020, 7, 266−272

Supporting Information

Light absorption by organic aerosol emissions rivals that of black carbon from residential biomass fuels in South Asia

Apoorva Pandey[1], Alice Hsu[1], Suresh Tiwari[2], Shamsh Pervez[3], Rajan K. Chakrabarty[1,*]

[1]Department of Energy, Environmental and Chemical Engineering, Washington University in St. Louis, Missouri – 63130, USA.

[2]Indian Institute of Tropical Meteorology, Pune 411008, India

[3]School of Studies in Chemistry, Pandit Ravishankar Shukla University, Raipur, Chhattisgarh 492010, India

* Correspondence to: *chakrabarty@wustl.edu*

Methods:

1. **Field sampling:** Experimental methods for the field study conducted between December 19th and 30th of 2015 in Chhattisgarh, India have previously been discussed in Pandey, et al. [1]. Test fuels included fuelwood, agricultural residue and cattle dung collected from different regions in India. All fuels were analyzed for elemental (carbon, oxygen, hydrogen, nitrogen) composition and moisture content. Each cooking test, involving the preparation of a local meal item, was conducted by a member (any one of five) of the research team which included several locally-based researchers familiar with the stove operation. Ignition was initiated using a small amount of dung (20-50 g) doused with ~10 ml kerosene and the test fuel was added after flaming conditions were established. The initial ten-minute period of the combustion cycle was termed the *ignition* phase. The remainder of the cooking cycle was designated as the *flaming* phase when a visible flame was present: re-kindling sometimes led to a diminished or nearly extinguished flame and these instances were categorized under ignition. When only glowing embers were present, combustion entered the *smoldering* phase. Two of the fuels (U.P. dung and Chh. rice straw) could not sustain the flaming phase for more than a few minutes. These fuels were therefore burned in combination with U.P. wood.

   The kitchen was a single room on the second floor of the house, separate from all other rooms. A permanently open door and a partially covered window covered were ventilation sources. Real-time instruments sampled naturally diluted emissions from an eight-armed stainless steel placed ~1.2 m above the top of the stove (Fig. S1). A Testo-350 gas analyser continuously measured carbon monoxide (CO) and carbon dioxide (CO_2) during the cooking tests. $PM_{2.5}$ samples were collected on 47 mm PTFE membrane and quartz fiber filters using Minivol (5 L min^{-1}) samplers (AirMetrics Model 4.2), during different times in each cooking cycle. Filter

sample durations ranged from 0.5 to 4 minutes to prevent filter overloading. Field blanks were collected (minimum sampling duration of 15 minutes) each day before testing. Wireless particle light scattering sensors (Sharp GP2Y) were attached to the Minivol sampler and the sampling probe during six experiments to check for any significant differences in the particle concentrations measured at the two locations. Measurements where either sensor was saturated were discarded, and a linear regression analysis performed on the valid data points. A correction factor of 1.6 was applied based on regression slope[11].

2. **Filter optical analysis:** PTFE filters were weighed before and after sampling using a microbalance at Pt. Ravishankar Shukla University, Raipur, India to obtain the net mass deposited. While in the test kitchen, the filter samples were kept in a portable insulated box with freezer packs. Both sets of filters were stored in a freezer (-20 ºC) after each day of sampling. Storage period (before analysis) was less than 50 days for all filters. At the end of the study, the quartz filters were transported to Desert Research Institute, Nevada, where they were analyzed using the Interagency Monitoring of Protected Visual Environments – A (IMPROVE_A) thermal-optical reflectance (TOR) method to determine elemental and organic carbon fractions in the sampled particulates. The PTFE filters were brought to Washington University in St Louis for optical analysis. For each filter, sample-side transmittance (T_s) and reflectance (R_s) were measured for wavelengths 350-900 nm using a Perkin-Elmer LAMBDA 35 UV-vis spectrophotometer (see Pandey, et al. [2] for more details on filter analysis technique).

Statistical and error analysis methods: We derived the bounds on all reported quantities from the distribution of values derived from individual samples. All results are reported as means ± standard deviations or along with 95% confidence intervals. Given that emissions data are non-negative and exhibit distributions with long tails (due to the occurrence of high

emissions events[1, 3]), a lognormal distribution was selected as a probable candidate for representing pooled absorption emission factor (AEF) data. We evaluated the assumption of lognormality of AEF data by performing the Anderson-Darling test on log(AEF): test statistic was calculated as 0.324 and the critical value at a significance level of 0.05 was 0.7408. The null hypothesis (that data are normally distributed) is rejected if the test statistic is larger than the critical value. Thus, in this case the null hypothesis was valid at a 0.05 significance level. Student's *t*-tests comparing AEFs for the three fuel categories (fuelwood, agricultural residue and dung) were also performed on log(AEF) instead of directly using AEF values.

Figures (S1-S6) and Table (S1):

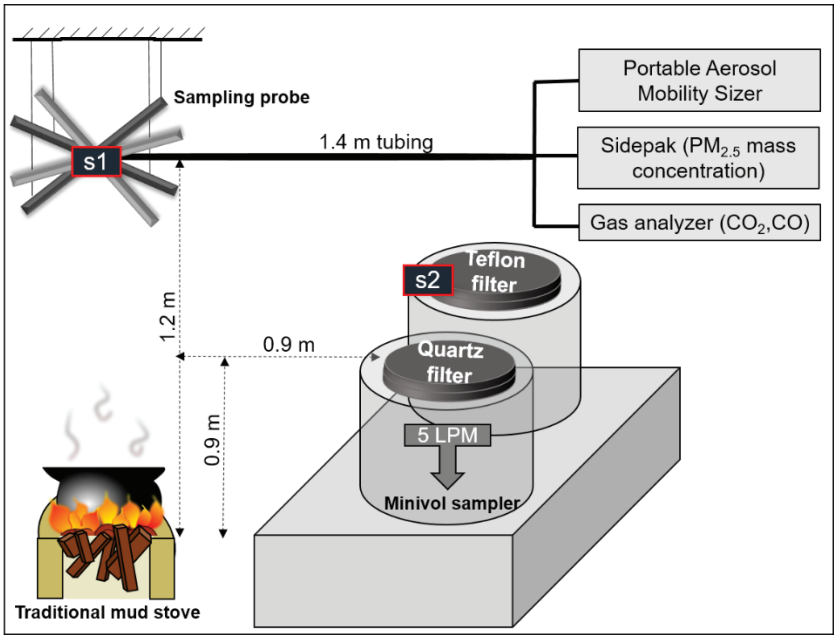

Fig. S1: Schematic representation of the experimental setup. S1 and S2 denote the position of the wireless optical sensors.

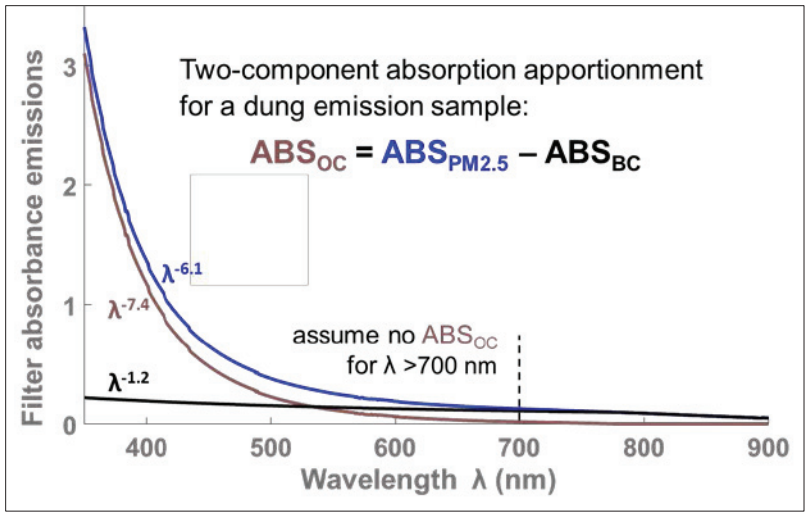

Fig. S2: Absorption spectrum for a sample of dung emissions is deconvoluted by assigning all absorption at wavelengths greater than 700 nm to BC and extrapolating BC absorption at smaller wavelengths using a fixed BC AAE (1.2 in the figure).

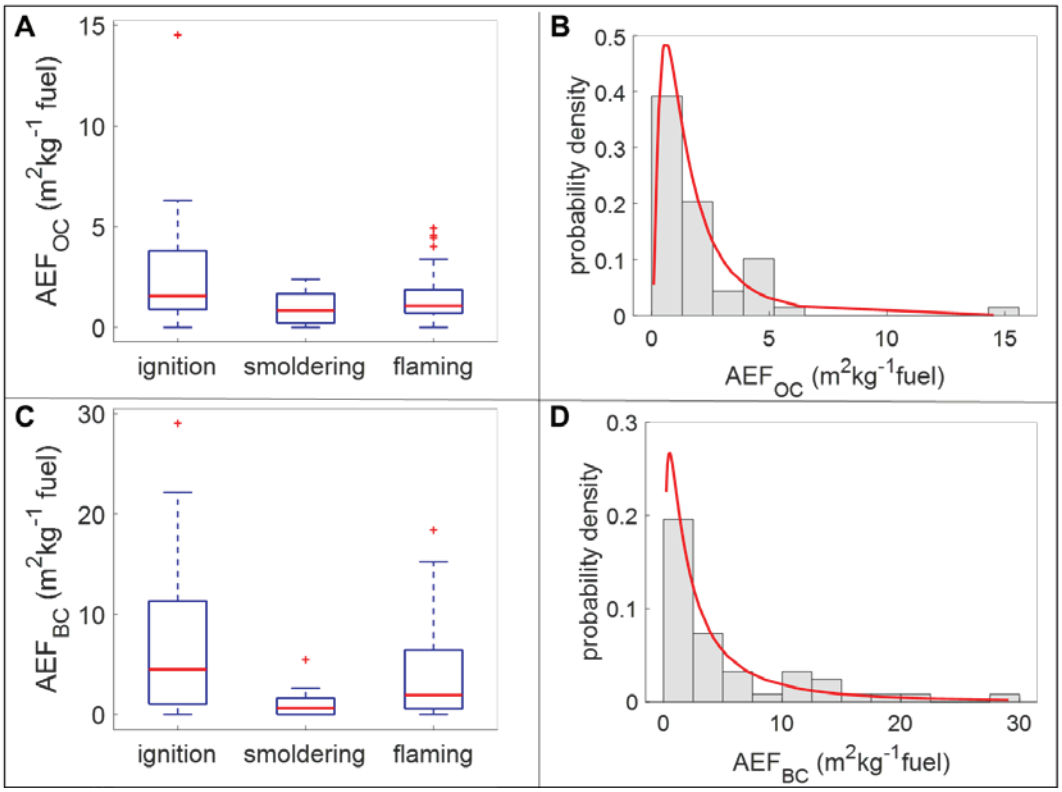

Fig. S3: Absorption emission factors in m^2kg^{-1} fuel consumed, at 550 nm wavelength: (A) AEF_{OC} grouped by observed combustion phase: boxes denote the upper and lower quartiles and whiskers denote 1.5 times the interquartile range, outliers are shown as red + symbols, number of samples for each category are specified above the whiskers and (B) AEF_{OC} shown as a histogram of all samples, overlaid by a fitted lognormal distribution. Plots in (C) and (D) are the same as (A) and (B), respectively, but for AEF_{BC}.

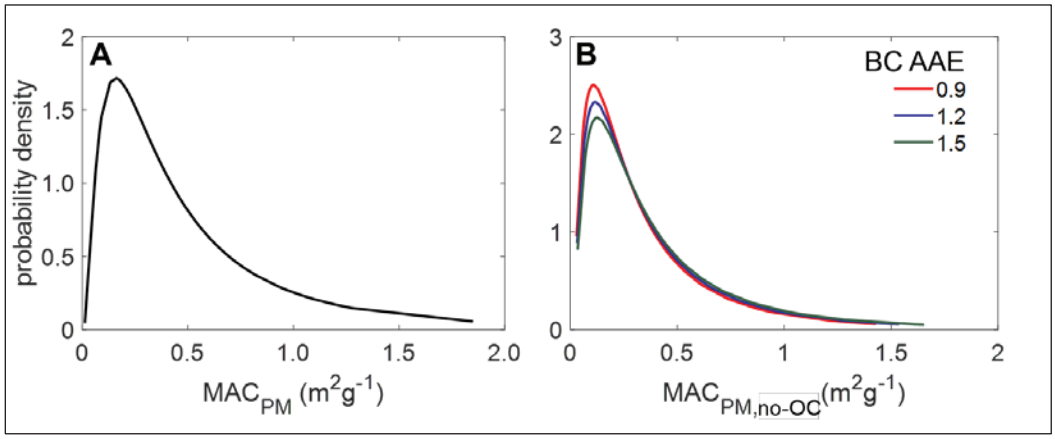

Fig. S4: Probability distributions of (A) MAC_{PM} and (B) $MAC_{PM,no\text{-}OC}$ for all samples in this study.

Table S1: Slope (m), intercept (c) and adjusted R^2 for the linear fits: $MAC_{PM,no\text{-}OC}$ =m* MAC_{PM} + c.

	BC AAE		
	0.9	1.2	1.5
m	0.82	0.88	0.94
c	-0.09	-0.09	-0.1
Adjusted R^2	0.97	0.97	0.97

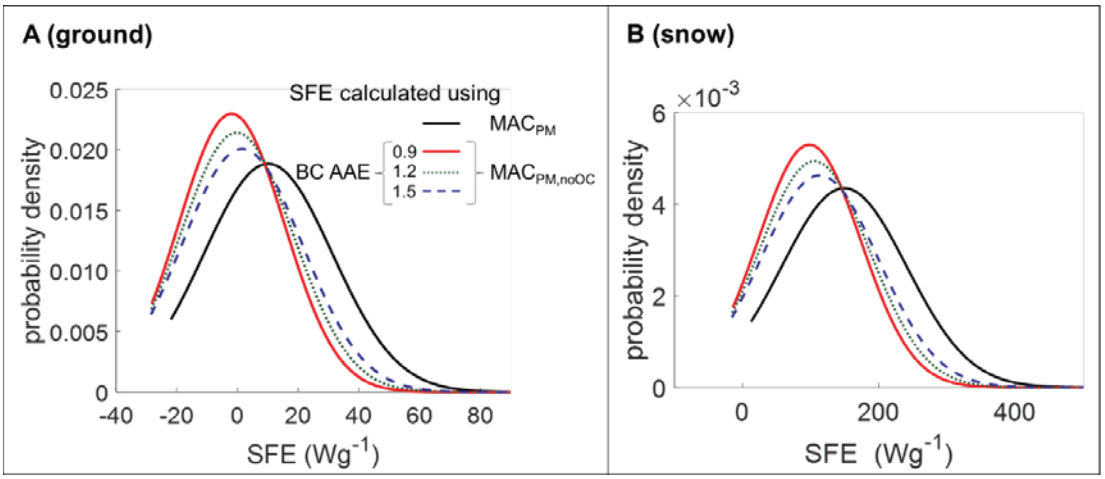

Fig. S5: Probability distributions of simple forcing efficiency of cookstove particulate emissions over (A) ground and (B) snow. Forcing was calculated with and without OC light absorption, with a fixed MSC =1.5 m^2g^{-1}.

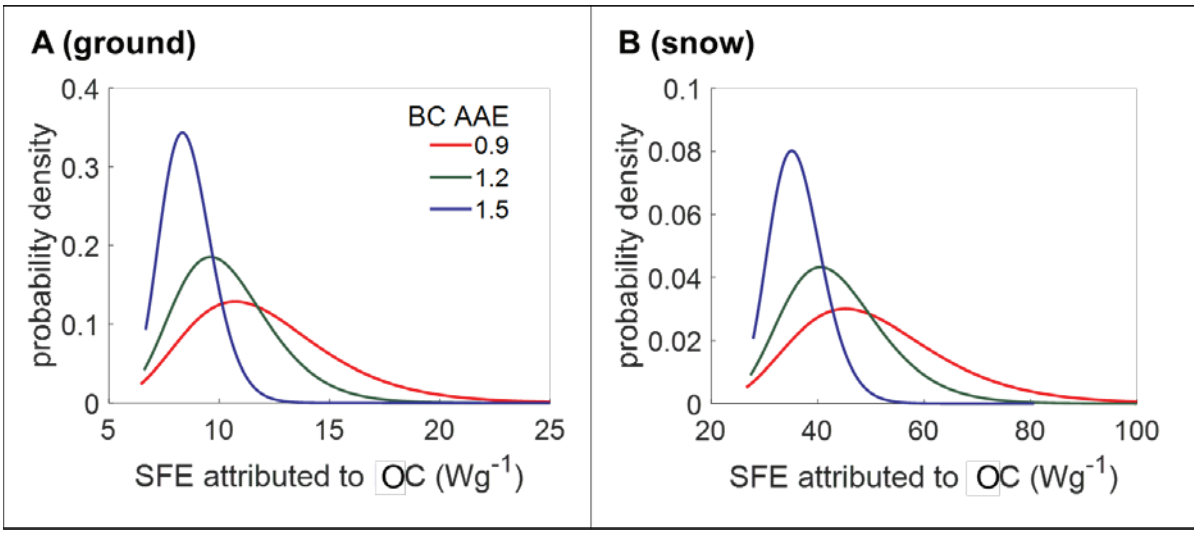

Fig. S6: Probability distributions of simple forcing efficiency of cookstove particulate emissions attributed to OC light absorption over (A) ground and (B) snow. The difference between SFE_{PM} and $SFE_{PM,no\text{-}OC}$ depends only the difference in the respective MAC values: $SFE_{PM} - SFE_{PM,noOC} = S(\lambda)\tau_{atm}^2(1 - Fc)\alpha_s \times \left[MAC_{PM}(\lambda) - MAC_{PM,noOC}(\lambda)\right]$ This difference can be interpreted as the contribution of OC light absorption to forcing by cookstove emissions.

References:

1. Pandey, A.; Patel, S.; Pervez, S.; Tiwari, S.; Yadama, G.; Chow, J. C.; Watson, J. G.; Biswas, P.; Chakrabarty, R. K., Aerosol emissions factors from traditional biomass cookstoves in India: insights from field measurements. *Atmos. Chem. Phys.* **2017,** *17*, (22), 13721-13729.
2. Pandey, A.; Shetty, N. J.; Chakrabarty, R. K., Aerosol light absorption from optical measurements of PTFE membrane filter samples: sensitivity analysis of optical depth measures. *Atmos. Meas. Tech.* **2019,** *12*, (2), 1365-1373.
3. Chen, Y.; Roden, C. A.; Bond, T. C., Characterizing biofuel combustion with patterns of real-time emission data (PaRTED). *Environ. Sci. Technol.* **2012,** *46*, (11), 6110-6117.